plants

MDPI

Article

Understanding Callus Types in Maize by Genetic Mapping and Transcriptional Profiling

Guifang Lin [1,2,†], Yan Liu [3,†], Tej Man Tamang [1,4,†], Yang Qin [3], Mingxia Zhao [1], Jun Zheng [3], Guoying Wang [3], Hairong Wei [5], Sunghun Park [6], Myeong-Je Cho [7], Frank F. White [8], Yunjun Liu [3,*] and Sanzhen Liu [1,*]

1 Department of Plant Pathology, Kansas State University, Manhattan, KS 66506, USA; guifanglin311@gmail.com (G.L.); ttamang@ycp.edu (T.M.T.); mingxia.zhao@pku-iaas.edu.cn (M.Z.)
2 Basic Forestry and Proteomics Research Center, Fujian Agriculture and Forestry University, Fuzhou 350002, China
3 State Key Laboratory of Crop Gene Resources and Breeding, Institute of Crop Sciences, Chinese Academy of Agricultural Sciences, Beijing 100081, China; lyer09@163.com (Y.L.); 82101231090@caas.cn (Y.Q.); zhengjun02@caas.cn (J.Z.); wangguoying@caas.cn (G.W.)
4 Environmental Horticulture, York College of Pennsylvania, York, PA 17403, USA
5 College of Forest Resources and Environmental Science, Michigan Technological University, Houghton, MI 49931, USA; hairong@mtu.edu
6 Department of Horticulture and Natural Resources, Kansas State University, Manhattan, KS 66506, USA; shpark@ksu.edu
7 Innovative Genomics Institute, University of California, Berkeley, CA 94704, USA; mjcho1223@berkeley.edu
8 Department of Plant Pathology, University of Florida, Gainesville, FL 32611, USA; ffwhite@ufl.edu
* Correspondence: liuyunjun@caas.cn (Y.L.); liu3zhen@ksu.edu (S.L.)
† These authors contributed equally to this work.

Abstract

Plant transformation efficiency is highly dependent on species, individual genotypes, and tissue types. In maize, immature embryos are regularly used for transformation. The process relies heavily on callus development, as it is intricately associated with somatic embryogenesis and subsequent plant regeneration, both of which directly affect transformation efficiency. Immature embryos of the segregation progeny derived from the two inbred parents, a transformation-amenable line A188 and a recalcitrant line B73, can be cultured to form two primary callus types: Type I and Type II. The Type II callus grows faster and is a favorable type for regeneration. Here, Type I and II calli from the B73xA188 F2 population were genotyped by Genotyping-By-Sequencing (GBS). Quantitative trait locus (QTL) analysis of the callus type identified QTLs at chromosomes 2, 5, 6, 8, and 9. The result was largely supported by the bulk segregant RNA-seq (BSR-seq) genetic analysis using RNA from separately pooled Type I and II calli. Both analyses revealed that an allele of A188 on chromosome 6 and B73 alleles on chromosomes 2, 5, 8, and 9 promoted the formation of the Type II callus. Differentially expressed genes (DEGs) between the Type II and I F2 calli were also identified. In addition, the A188 calli developed from the same immature embryos often exhibit heterogeneous morphology, including the fast- and slow-growing callus sectors. The transcriptional comparison between the two sectors was performed to identify DEGs. Both sets of DEGs were enriched in genes involved in cell-wall organization and wax biosynthesis pathways.

Keywords: regeneration; plant transformation; culturability; maize

check for updates

Academic Editor: Shri Mohan Jain

Received: 24 August 2025
Revised: 23 September 2025
Accepted: 11 October 2025
Published: 15 October 2025

Citation: Lin, G.; Liu, Y.; Tamang, T.M.; Qin, Y.; Zhao, M.; Zheng, J.; Wang, G.; Wei, H.; Park, S.; Cho, M.-J.; et al. Understanding Callus Types in Maize by Genetic Mapping and Transcriptional Profiling. *Plants* **2025**, *14*, 3168. https://doi.org/10.3390/plants14203168

Copyright: © 2025 by the authors. Licensee MDPI, Basel, Switzerland. This article is an open access article distributed under the terms and conditions of the Creative Commons Attribution (CC BY) license (https://creativecommons.org/licenses/by/4.0/).

1. Introduction

Plant transformation is an essential technique for genome engineering, and efficient transformation protocols for diverse genetic backgrounds are desirable [1,2]. Maize transformation efficiency has been improved through genetic improvement [3], medium optimization [4–7], and morphogenic gene manipulation [8–10]. However, the transformation efficiency across cultivars or genotypes varies dramatically, and the underlying genetic basis remains largely unknown [1,2].

Immature embryos are often used as explants for DNA transformation in maize. Callus formation, somatic embryogenesis, and tissue regeneration are the major factors influencing the transformation efficiency [4,11,12]. Of 25 maize inbred lines surveyed, calli induced from immature embryos from A188, A634, W117, MS71, and H99 were highly regenerable, whereas the regeneration frequencies of calli from B73, H84, and N28 were low [12]. When crossed with A188, the regeneration efficiency of progeny of regeneration-recalcitrant lines B73, Mo17, H95, Oh43, and VA26 was markedly improved, indicating that A188 contains some dominant alleles for high regeneration ability [12].

Type I and Type II calli are two distinct embryogenic callus types that can be initiated from maize immature embryos. A Type I callus is translucent, typically slow growing, and of a compact structure mixed with differentiated tissue, while a Type II callus is white or pale yellow, fast growing and friable [11,13–16]. Most maize genotypes primarily produce a Type I callus [17]. While both Type I and II calli from different genotypes have been used to produce transgenic plants, the Type II callus is considered favorable for gene transformation due to its rapid growth and high regeneration efficiency [14,15,17–19].

Hi-II is a maize line with a high transformation efficiency [2,19,20]. Hi-II was generated from a cross of two partial inbred lines, Hi-II A and B, both of which exhibited nearly total Type II callus initiation from immature embryos [3,19,20]. Hi-II A and B were independently developed from crosses between B73, a transformation-recalcitrant elite breeding line, and A188, a highly regenerable line with poor agronomic qualities [12,21]. Type II calli occur upon culture of immature embryos from both A188 and B73 genotypes. However, the frequency of a Type II callus from B73 is very low [18].

The genetic basis of maize callus types is unknown. At the same time, high Type II callus initiation of Hi-II A and B and the benefit of crossing low regeneration lines with A188 support the possibility of callus regeneration improvement through genetic selection. Previously, a cross of B73xA188 was generated and backcrossed six generations to B73 (BC6), and individuals with the highest frequency of Type II callus were selected from each generation [22]. A single BC6 line was self-pollinated for four generations (BC6S4). The BC6S4 line carries five segments of A188 on chromosomes 1, 2, 3, and 9 on the basis of genotyping data of 73 RFLP markers. In a separate study, 89 genetic markers were used to identify culturability-associated regions on chromosomes 1, 3, 6, and 10 using progeny of Hi-II and a commercial inbred line FBLL [23]. A study of recombinant inbred lines of Mo17xH99, another low and high transformation efficient line cross, found QTLs related to callus formation at chromosomes 1, 2, 3, 5, 6, and 8 using 111 genetic markers [24]. A tissue culture response QTL between A188 and B73 was mapped to a region between around 164.8 Mb and 166.8 Mb on chromosome 3 (B73v3) [25]. A Wuschel-like homeobox 2a (*WOX2a*) gene enhancing maize regeneration was recently identified in the QTL region [26]. Overall, previous QTL studies were limited by the number of markers and segregating individuals.

Here, out of more than two thousand calli generated using immature embryos from self-pollinated B73xA188 F1 plants, distinct Type I and Type II F2 calli were collected for genetic mapping and transcriptomic profiling. Transcriptomic analysis was also performed on fast- and slow-growing callus sections of heterogeneous callus tissues of A188. Integration of genetic and transcriptomic data identified candidate genes that may be involved in callus development.

2. Results

2.1. Genetic Mapping of the Callus Type

Immature embryos (N = 2194) dissected from 13 self-pollinated B73xA188 F1 plants were cultured to select 100 XT-I and 100 XT-II calli [27]. One half of each individual XT-I or XT-II callus was subjected to Genotype-By-Sequencing (GBS). The other half of each callus was pooled into two XT-I and two XT-II bulks, with 50 calli per bulk for BSR-seq analysis.

GBS data were successfully generated for 153 individual calli, including 79 XT-I and 74 XT-II calli. Analysis of GBS data led to the identification of 96,703 SNPs. The SNP genotypes of each F2 individual callus were used to infer chromosomal segments harboring multiple SNP markers with the same genotypes (Supplementary Data S1). The number of segments per F2 individual represented the number of discernible recombination events. After filtering F2 individuals with recombination events higher than expected, 60 XT-I and 58 XT-II individuals were retained [28]. In total, 6369 GBS segment markers were generated for genetic mapping of the callus type (Figure 1A,B; Table 1). For the QTL mapping, a standard interval QTL mapping approach and a method of logistic regression were employed (Figure 1C, Supplementary Data S2). Concordant QTL peaks were identified by standard QTL and logistic regression on chromosomes 2, 5, 6, 8, and 9, which were designated as ctAB2a, ctAB5a, ctAB6a, ctAB8a, and ctAB9a, respectively (Table 1). The five QTLs explained 50.9% of the phenotypic variance. The LOD-supported QTL intervals were estimated, resulting in broad genomic ranges of the QTL intervals.

BSR-seq analysis of bulked XT-I and XT-II samples revealed 68,147 SNPs in the F2 population. Assuming read counts of two alleles of a SNP site followed a binomial distribution, the statistical test found 284 SNP sites associated with a divergent allele distribution in XT-I and XT-II pooled samples. Most associated SNPs were also located on chromosomes 2, 5, 6, 8, and 9 (Figure 1D; Table 1, Supplementary Data S3).

Table 1. The QTLs supported by three mapping methods.

QTL	chr	R/qtl		Logistic Regression		BSR-seq		QTL Interval (bp) *	
		Pos (bp)	LOD	Pos (bp)	*p*-Value	Pos (bp)	*p*-Value	Start	End
ctAB5a	5	169,273,698	6.9	169,273,698	1.7×10^{-7}	84,632,155	0.0×10^{0}	80,458,296	198,270,432
ctAB8a	8	174,632,571	4.6	174,479,910	2.4×10^{-5}	169,073,812	1.5×10^{-9}	127,872,514	180,929,814
ctAB6a	6	88,567,616	4.1	83,296,319	9.6×10^{-5}	99,960,681	1.1×10^{-12}	1,006,642	100,419,946
ctAB2a	2	158,183,928	3.8	99,580,047	1.9×10^{-4}	156,883,753	3.9×10^{-10}	24,095,104	176,011,606
ctAB9a	9	108,566,128	3.3	159,752,864	4.5×10^{-4}	108,540,812	4.4×10^{-11}	10,213,832	158,723,248

* The interval was the LOD support interval, and CtAB.5.01 was adjusted to include the BSR-seq peak.

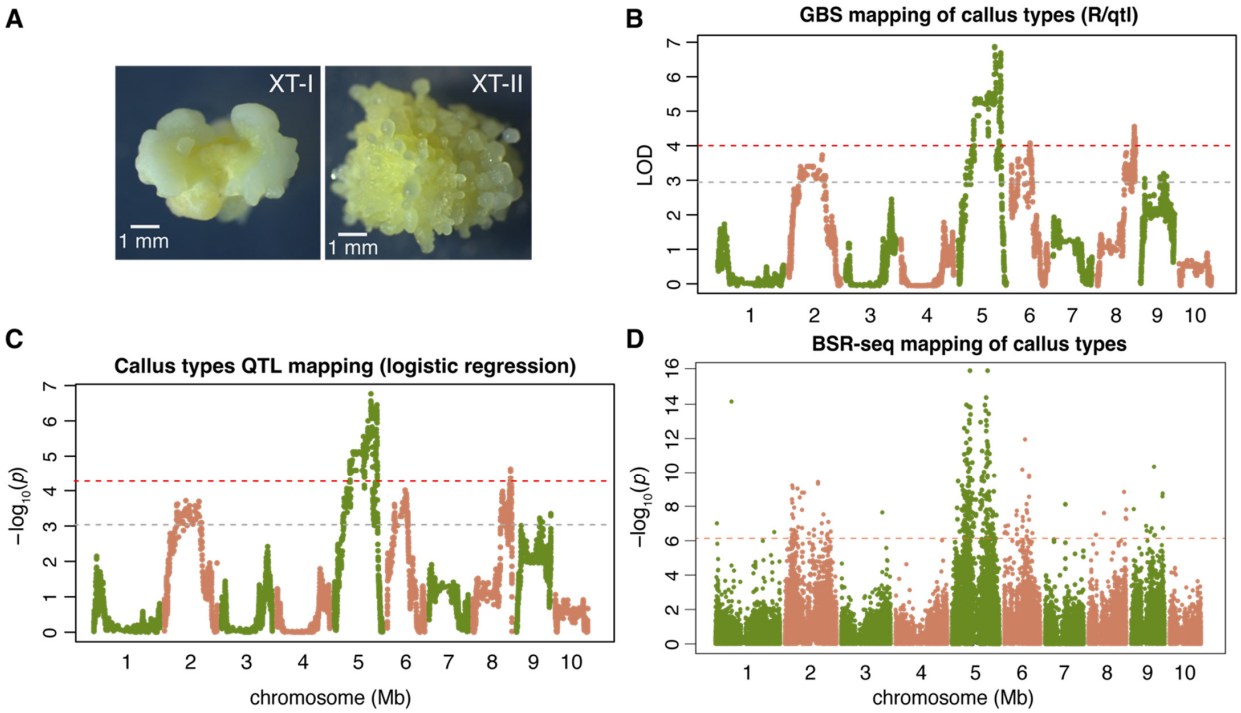

Figure 1. Genetic mapping of callus type QTLs. (**A**) Type I and II calli initiated from B73xA188 F2 I immature embryos. (**B**) Genetic mapping of the callus type using the standard interval mapping with a binary model. The red dash line indicates the significance threshold defined by the 1000 permutation tests at 5% significance level, and the gray dash line indicates the LOD threshold of 3. (**C**) The result of genetic mapping with a logistic regression method. The red dash line indicates the threshold defined by the 1000 permutation tests at the 5% significance level, and the gray dash line indicates the false discovery rate threshold of 0.01. (**D**) Genetic mapping of callus types via BSR-seq. The dash line indicates the threshold using the Bonferroni correction at the 5% significance level.

2.2. Alleles Contributing to Type II Callus Formation

Among the five QTLs, ctAB6a was the only QTL where the A188 genotype positively contributed to the Type II callus (Figure 2). QTL ctAB6a was located in a region of approximately 10 Mb to 100 Mb on chromosome 6 (Figure 2A,B). The distribution of three segregating genotypes showed that the A188 and B73 homozygous genotypes at the ctAB6a interval were enriched in XT-II and XT-I callus samples, respectively (Figure 2C,D). The heterozygous genotype was not strongly selected in either XT-I or XT-II, indicating non-dominant allelic impacts on callus types. QTL ctAB5a was the strongest QTL, which was mapped in the interval of 80 Mb to 198 Mb (Table 1, Figure 3A,B). The homozygous A188 and B73 genotypes of ctAB5a were enriched in XT-I and XT-II individuals, respectively, indicating that the B73 allele was favorable for the Type II callus (Figure 3C,D). Similar to QTL ctAB6a, the heterozygous genotype at QTL ctAB5a was not strongly selected in either XT-I or XT-II, indicative of non-dominant allelic impacts on callus types. In addition to ctAB5a, the B73 alleles were favorable alleles for Type II callus phenotype at the QTLs of ctAB2a, ctAB8a, and ctAB9a (Figures S1–S3; Table 1). The phenotypic means of the three genotypes at all these four QTL peaks indicated that two alleles of all QTLs did not function in a dominant manner (Figure S4). Although we did not identify the chromosome 3 QTL that was previously mapped to condition tissue culture responses, we found that the B73 allele was under-represented in both XT-I and XT-II samples (Figure S5) [25]. A good proportion of individuals with the heterozygous genotype in both callus types indicated the impact from the A188 allele at the chromosome 3 locus on the tissue culture response was dominant (Figure S5).

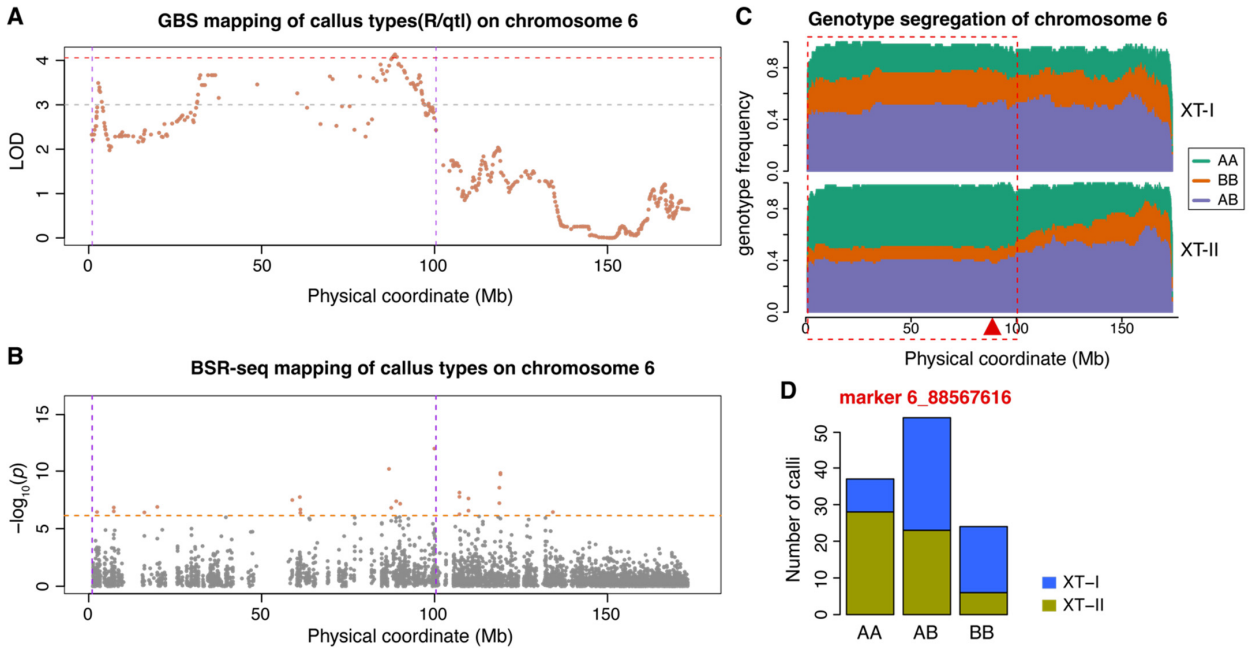

Figure 2. Detailed characterization of QTL ctAB6a. (**A**) Genetic mapping of callus types with GBS segment markers on chromosome 6. The red dash line indicates the significance threshold defined by permutation tests at the 5% significance level, and the gray dash line indicates the LOD threshold of 3. (**B**) Genetic mapping of callus types from BSR-seq. The orange dash line indicates the threshold defined by the Bonferroni correction at the 5% significance level. The significant SNP markers are colored in green. The vertical purple dash lines (in both (**A**) and (**B**)) indicate the LOD support QTL interval, and the red vertical dash line indicates the left flanking of the interval adjusted based on the BSR-seq mapping. (**C**) The distribution of genotypes of the 60 XT-I F2 calli and 58 XT-II F2 calli on chromosome 6. The red rectangle box indicates the QTL interval, and the red triangle points to the QTL peak. (**D**) Distribution of callus types in three genotypes. AA: A188 homozygous genotype; BB: B73 homozygous genotype; AB: heterozygous genotype.

2.3. Type II Callus Favorable Alleles of Many QTLs Were Selected in Both Hi-II A and B

Two highly culturable, nearly inbred lines selected from the progeny of A188 and B73, Hi-II A and B, were also subjected to GBS genotyping. Chromosomal segments of Hi-II A and B were inferred by GBS genotypes, showing that most chromosome regions were homozygous (Figure 4). Based on genotypes of segments, 22 and 54 recombination breakpoints were found in Hi-II A and B, respectively (Figure 4). Although Hi-II A and B were developed from independent F2 calli [3], the two lines shared genotypes of most chromosomal segments. The genotyping data showed that the Type II-callus-favorable B73 alleles at three QTLs, ctAB2a, ctAB6a, and ctAB8a, were selected in both Hi-II A and B. However, the Type II-callus-favorable B73 alleles at the major QTL, ctAB5a, and a minor QTL, ctAB9a, were not present in either line. Notably, both Hi-II A and B had the A188 genotype on the chromosome 3 QTL affecting tissue culture responses [25].

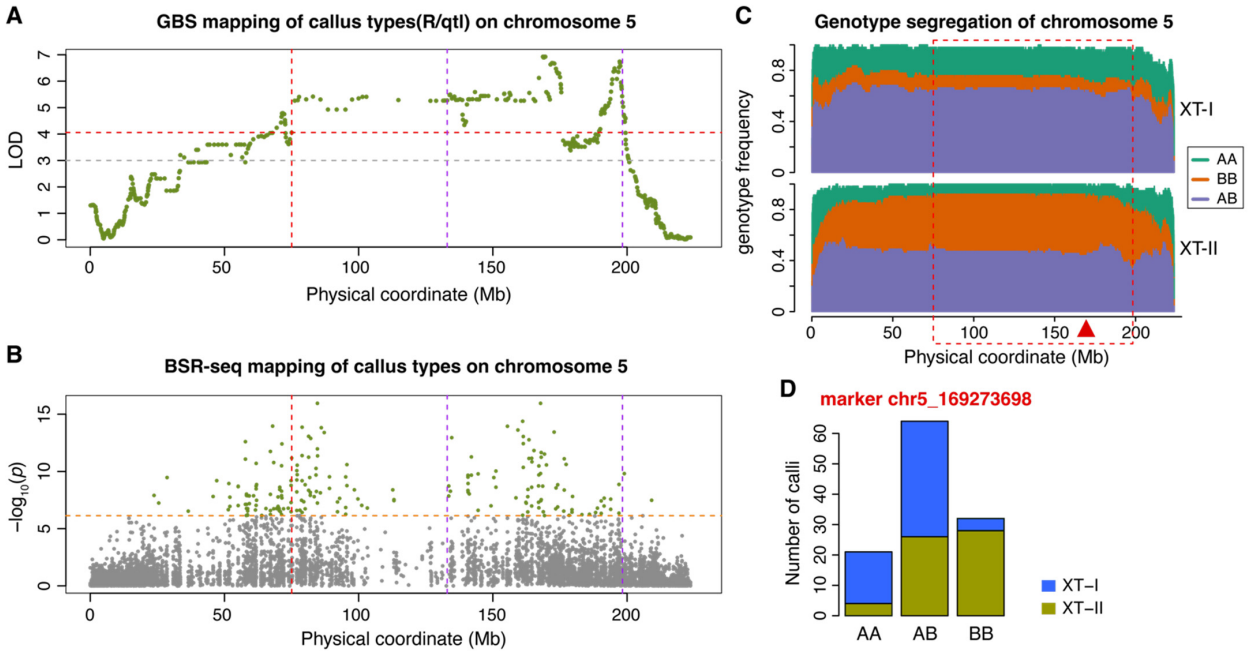

Figure 3. Detailed characterization of QTL ctAB5a. (**A**) Genetic mapping of callus types with GBS segment markers on chromosome 5. The red dash line indicates the significance threshold defined by permutation tests at the 5% significance level, and the gray dash line indicates the LOD threshold of 3. (**B**) Genetic mapping of callus types from BSR-seq. The orange dash line indicates the threshold defined by the Bonferroni correction at the 5% significance level. The significant SNP markers are colored in green. The vertical purple dash lines (in both (**A**) and (**B**)) indicate the LOD support QTL interval, and the red vertical dash line indicates the left flanking of the interval adjusted based on the BSR-seq mapping. (**C**) The distribution of genotypes of the 60 XT-I F2 calli and 58 XT-II F2 calli on chromosome 5. The red rectangle box indicates the QTL interval, and the red triangle points at the QTL peak. (**D**) Distribution of callus types in three genotypes. AA: A188 homozygous genotype; BB: B73 homozygous genotype; AB: heterozygous genotype.

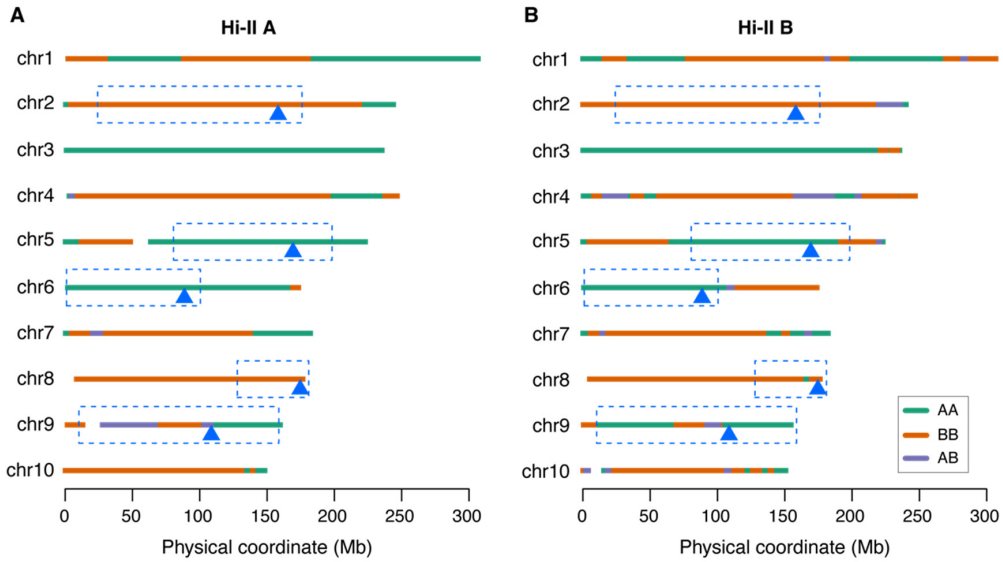

Figure 4. Genotypes of Hi-II A and B. (**A**,**B**) Genotype origins of chromosomal segments in Hi-II A (**A**) and B (**B**). The triangle under chromosomes labels the peak location of the QTLs, and the color of the triangle indicates the favorable allele. Green indicates the A188 allele, and orange indicates the B73 allele. Blue dotted rectangles indicate the QTL intervals. AA: A188 homozygous genotype; BB: B73 homozygous genotype; AB: heterozygous genotype.

2.4. Differential Expression Between Different Types of Calli

Gene expression analysis between XT-II and XT-I calli identified 928 up-regulated and 753 down-regulated differentially expressed genes (DEGs) in XT-II as compared to XT-I (Supplementary Data S4 and S5). Enrichment analysis of GO terms in biological process and molecular function domains indicated that up-regulated genes were enriched in the pathways related to oxidant detoxification, stress response, biosynthesis of cell-wall components (cutin and wax), and heme binding, while the down-regulated genes were enriched in the pathways involved in transcription factor (TF) activity, transmembrane transport, protein dimerization, and nicotianamine metabolism (Figure 5A,B). In fast- and slow-growing calli, 935 up-regulated DEGs and 1509 down-regulated DEGs in fast-growing calli were identified in comparison to slow-growing calli (Figure S6). GO Enrichment analysis in the biological process and molecular function domains indicated that up-regulated DEGs were enriched in the process related to transcriptional regulation factors, transmembrane transport, wax and suberin biosynthesis, and hormone response. The down-regulated DEGs were enriched in the process of oxidative response, heme binding, response to oxidative stress, gibberellin 2-beta-dioxygenase activity, and cell-wall macromolecules (Figure 5C,D). The two differential expression analyses identified common TF DEGs. Eight TF genes were up-regulated in Type II and fast-growing calli as compared to Type I and slow-growing calli, respectively (Figure 5E). The up-regulated genes included two genes in the WOX family, Zm00001d039017 (*wox9c*) and Zm00001d043937 (*wox9b*), and two genes in the MYB family, Zm00001d043131 (*myb138*) and Zm00001d041853 (*myb8*). Note that both Zm00001d039017 and Zm00001d043937 were highly expressed in embryos, particularly in immature embryos, based on the publicly available expression atlas from MaizeGDB, while the two genes encoding MYB did not show this pattern (Figures S7–S10) [29,30]. Conversely, 15 TF genes were down-regulated in Type II and fast-growing calli, including six genes from the ERF family and three genes from the bHLH family (Figure 5F).

Genes in biosynthesis of wax and fatty acid were enriched in the up-regulated DEGs. Detailed examination of the wax pathway found that five out of eight genes involved in the biosynthesis and transportation of cuticular wax were up-regulated in the Type II callus as compared to the Type I callus. These five genes include *gl2* (Zm00001d002353), *gl6* (Zm00001d041578), *gl8* (Zm00001d017111), *gl13* (Zm00001d039631), and *gl14* (Zm00001d004198) (Figure 6). Among these, the wax transmembrane transporter gene *gl13* [31] and a gene with unknown function *gl14* [32] were also up-regulated in the fast-growing calli as compared to the slow-growing calli.

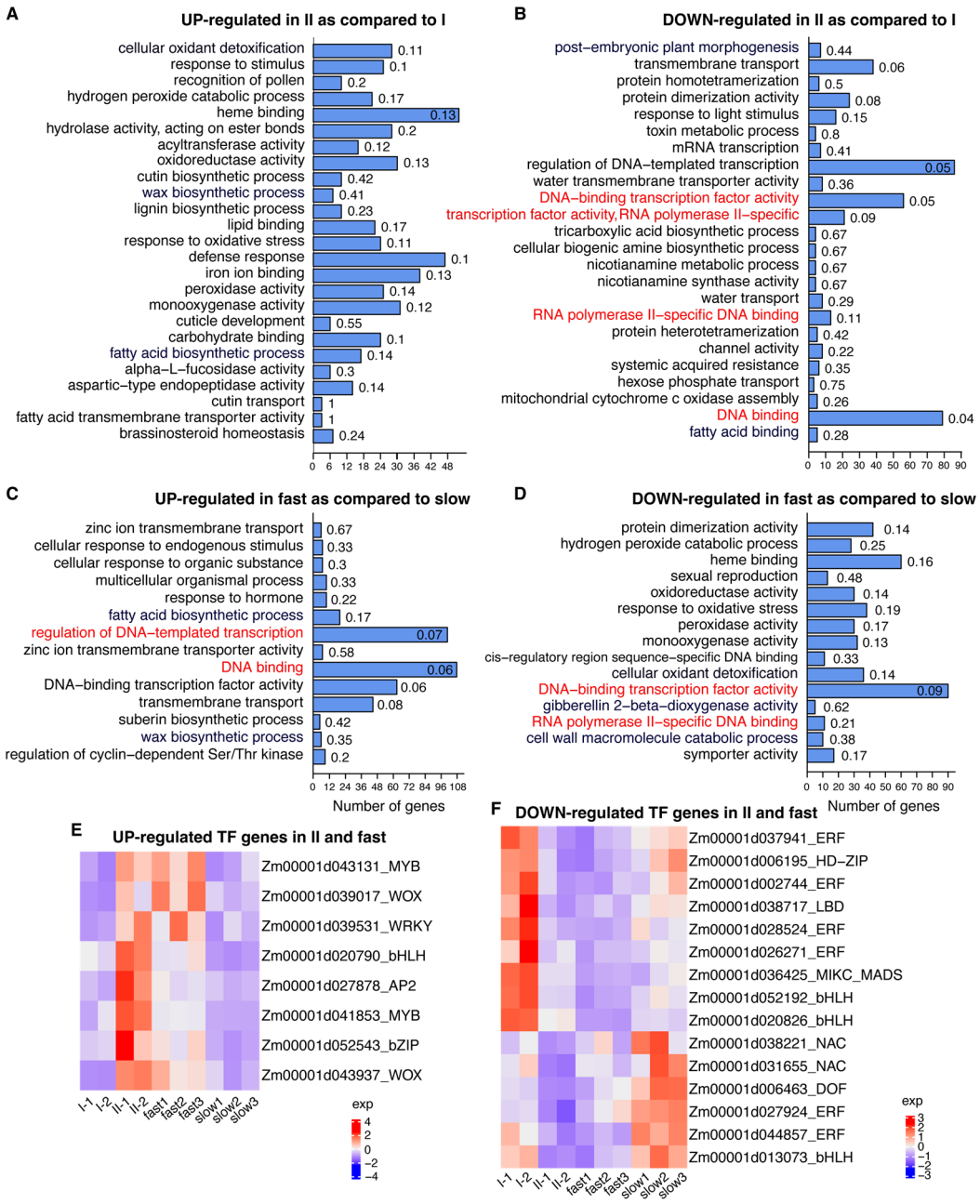

Figure 5. Enrichment of gene ontology (GO) in DEGs and expression of TF genes. (**A**,**B**) GO enrichment analysis of up- and down-regulated DEGs in XT-II (II) as compared to XT-I (I). (**C**,**D**) GO enrichment analysis of up- and down-regulated DEGs in fast-growing calli as compared to slow-growing calli. Each number on the top of a bar is the proportion of DEGs in the total genes of a certain GO. Red highlights GO terms related to transcription factor (TF) activities. (**E**) Heatmap of standardized expression of TFs that were up-regulated in XT-II as compared to XT-I and up-regulated in fast-growing calli as compared to slow-growing calli. (**F**) Heatmap of standardized expression of TFs that were down-regulated in XT-II as compared to XT-I and down-regulated in fast-growing calli as compared to slow-growing calli.

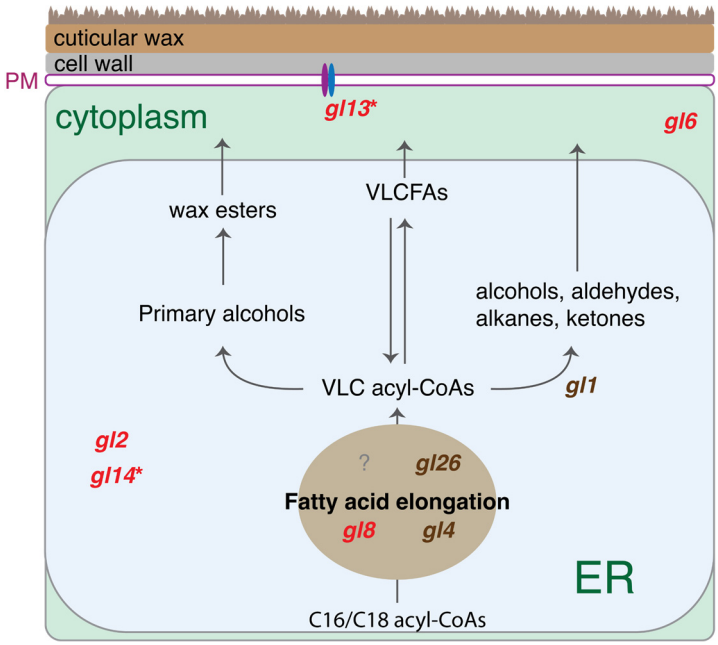

Figure 6. Genes in the pathway of cuticular wax production. The wax biosynthesis pathway was adapted from Figure 1B in Lewandowska et al. 2000 [33]. Very-long-chain fatty acids are produced and modified in the ER by various enzymes, resulting in wax components, which are then deposited to the plant surface through transmembrane transporters (e.g., GL13). Genes that are red-highlighted were up-regulated in the Type II callus as compared to the Type I callus. Two genes (*gl13* and *gl14*) labeled by an asterisk were up-regulated in the fast-growing callus as compared to the slow-growing callus. Genes that are brown-highlighted were not differentially expressed in both comparisons. VLCFA: very-long-chain fatty acid; VLC: very-long-chain; ER: endoplasmic reticulum; and PM: plasma membrane.

2.5. Integration of Genetic Mapping and DEGs

The QTL intervals included 21 DEGs that were up-regulated in XT-II and fast-growing calli as compared with XT-I and slow-growing calli, respectively, and 28 DEGs that were down-regulated in XT-II and fast-growing calli (Supplementary Data S6). Of these 49 DEGs, six are in the interval of ctAB6a where the A188 allele type favored the formation of the Type II callus. One gene, Zm00001d036241 encoding GDSL esterase/lipase, was up-regulated, and five genes were down-regulated in both XT-II and fast-growing calli. Zm00001d036241 is presumably involved in lipid metabolism [34]. The five genes down-regulated in XT-II and fast-growing calli include *wat1* (walls are thin 1, Zm00001d036123) and *end1* (early nodulin homolog1, Zm00001d036125), which are homologs of genes involved in the nodule development, *si1* (silky1, Zm00001d036425) encoding a DNA binding protein relevant to the silk development, the gene Zm00001d036409 encoding an unknown function protein with C2-C2 zinc finger, and the gene Zm00001d035556 with an unknown function. Comparison of the A188 and B73 allele sequences found all these genes, except *si1*, exhibited nonsynonymous polymorphisms in exons.

The gene *wat1*, encoding an EamA-like transporter, was further examined. Comparison between the A188 and B73 allele sequences through Homotools [35] found two large insertions/deletions in the fourth intron and the 3′ untranslated region (3′ UTR), as well as three polymorphisms altering the protein product occurring in the fourth and fifth exons (Figure S11).

3. Discussion

Here, genomic loci associated with callus type were mapped to chromosomes 2, 5, 6, 8, and 9. Three of the QTLs mapped closely to previously reported QTL regions on chromosomes 2, 6, and 9 [2,3]. Alleles of the five QTLs favoring Type II calli were found in both A188 and B73 parents. The finding that the recombinant inbred lines (e.g., Hi-II A and B) developed a higher proportion of Type II calli than either parent during tissue culture indicated a combinational effect of the positive alleles. An allele of the QTL on chromosome 6 in A188 is associated with the Type II callus and may correspond with a previously reported regeneration-related QTL on chromosome 6 [23]. Our QTL analysis with GBS genotyping data of individual calli did not identify the chromosome 3 QTL or its associated *WOX2a* gene [25,26]. The failure to detect this QTL in our genetic analysis of F2 calli indicates that the chromosome 3 locus may not contribute to the determination of the callus type. Possibly, the QTL positively contributes to the regeneration ability of A188 and was not measured by our strategy. Although B73 does not carry this regeneration-favorable allele on chromosome 3, B73 has alleles favorable to Type II calli at multiple loci. In both Hi-II A and B lines, which form nearly 100% Type II calli and are highly regenerable, the chromosome 3 allele of A188 was selected with the addition of Type II-favorable alleles from A188 at ctAB06a and B73 at ctAB02a and ctAB08a. The combination of these alleles is, therefore, likely crucial for the regenerable lines from the progeny of A188 and B73.

Differential transcription comparisons between Type II and Type I calli, and between the fast- and slow-growing A188 calli, revealed that the genes in the pathway related to the cell-wall organization were enriched. One gene, *wat1* (Zm00001d036123), is located in the region of a QTL on chromosome 6. In *Arabidopsis*, *wat1* is involved in secondary cell-wall thickness [36]. Mutations in *Arabidopsis wat1* result in defective cell elongation due to abnormal secondary cell-wall formation in the fiber cells, leading to short stems. A *wat1* homologous gene was a susceptibility gene to a Gram-positive bacterium in tomato, which was thought to be functional through reducing auxin and ethylene content in plants [37]. The involvement of *wat1* in the production of phytohormones and their impacts on callus development needs further exploration. The cell wall plays an important role in plant development [38], and the DEGs other than *wat1* involved in cell-wall organization were identified here and in a previous transcriptomic study of callus induction in maize [39]. Down-regulation of genes in cell-wall pathways could lead to loosening of the cell wall and, possibly, cellular adhesion [38,40,41]. The difference in the cell-wall component and structure between Type I and II calli may result in variations in their ability to uptake water, oxygen, and nutrients, thereby affecting the growing rate and regeneration ability.

Transcriptomic comparisons between Type II and Type I calli and between the fast- and slow-growing A188 calli revealed an enrichment of TFs both as up-regulated and down-regulated DEGs. Up-regulated DEGs included members of the MYB and WOX families. The MYB TF Zm00001d043131, referred to as MYB138, was previously implicated in callus induction [42]. A T-DNA insertion mutant of the *myb138* homologous gene reduced callus formation as compared with the wildtype in *Arabidopsis*, presumably through enhancing gibberellin transduction, and promotes differentiation [42]. The *myb138* gene was up-regulated in fast-growing and Type II tissues, indicating that MYB138 may promote cellular proliferation and callus formation. The transcriptomic comparisons also identified two up-regulated genes encoding WOX TFs up-regulated in both fast-growing and Type II calli. In addition, one *ERF* gene was up-regulated, while six *ERF* genes were down-regulated in both fast-growing and Type II callus tissues. Multiple WOX and ERF TFs have been demonstrated to play critical roles in embryogenesis and stem cell maintenance in plants [43].

From the transcriptional analysis, genes in the fatty acid biosynthesis pathway are markedly enriched in the DEGs from the two RNA-seq analyses related to the callus type and callus growth. Very-long-chain fatty acids (VLCFAs), fatty acids with at least 20 carbons, are the precursors of many lipids, cuticular waxes, suberins, sphingolipids, and phospholipids [44]. In maize, a dozen genes, referred to as glossy genes, responsible for production or secretion of cuticular waxes have been cloned [32]. Although multiple glossy genes were up-regulated in Type II calli as compared to Type I calli and/or up-regulated in fast-growing calli as compared to slow-growing calli, no evidence supports that *gl4*, a carbon-condensing enzyme catalyzing a rate-limiting step in VLCFA biosynthesis [45], was up-regulated. Nevertheless, the expression elevation of the transmembrane transporter gene *gl13* [31] and other fatty acid modifiers indicates the alteration of intracellular VLCFA compositions. VLCFAs have been demonstrated to confine callus formation in *Arabidopsis* [46]. The reduction of VLCFAs could elevate the level of cytokinin, which fine-tunes cellular proliferation [47]. Further, altered VLCFAs may influence the production of ethylene [48]. Many ERF-encoding TF genes were down-regulated in the Type II and fast-growing callus tissues, which indicates the possibility of decreased levels of ethylene. In the future, monitoring amounts and compositions of VLCFAs in different types of callus tissues will provide better understanding of the roles of VLCFAs in the production of cytokinin and ethylene in the maize callus, and importantly, their impact on the signaling regulation of cell proliferation and regeneration.

Multiple genomic strategies have been employed to understand the genetic basis of the formation of the callus type in B73xA188. By combining genetic mapping and transcriptional analysis to gain deeper insights into the genetics underlying the formation of different callus types, we identified a set of DEGs, particularly those encoding TFs, with some located within broad QTL intervals, providing the candidate genes for functional validation. In the future, testing some DEGs through ectopic expression (e.g., *wox9b* and *wox9c*) or knockout (e.g., *wat1*) could further translate our findings for improving callus formation, somatic embryogenesis, and regeneration in tissue culture recalcitrant maize lines.

4. Materials and Methods

4.1. Establishment of B73xA188 F2 and A188 Calli

B73xA188 F_1 plants were self-pollinated, and immature embryos (1.0–1.2 mm in length) were collected from 13 ears of 13 F2 plants at 11 days after pollination (DAP). Embryos were cultured in the dark at 28 °C for three weeks on N6 medium supplemented with 1.5 mg/L 2,4-dichlorophenoxyacetic acid (2,4-D) [49]. Out of 2194 total calli, 100 extremely Type I (XT-I) and 100 extremely Type II (XT-II) calli were selected. Each selected callus was bisected: one half was used for Genotyping-by-Sequencing (GBS), and the other for Bulked Segregant RNA-sequencing (BSR-seq). For BSR-seq, two biological replicates per callus type were generated, each consisting of 50 pooled calli, resulting in four total samples [50].

For the A188 line, 330 immature embryos were harvested from four ears at 11 DAP and cultured on N6 medium supplemented with 1.5 mg/L 2,4-D for 30 days, followed by subculture for 5 days. Type II calli from A188 often exhibited distinguishable fast- and slow-growing sectors upon closer inspection. These sectors were dissected from 20 representative calli and pooled into fast- and slow-growing bulks. Three biological replicates were collected for each callus growth type and subjected to RNA-seq.

4.2. DNA Isolation and GBS Sequencing

Leaves of ten-day seedlings from each maize line were collected for DNA extraction using the DNeasy Plant Mini Kit (Qiagen, Hilden, Germany). DNA samples were dissolved in water and normalized to 15 ng/μL for GBS library preparation.

A modified version of a previously published GBS protocol using the restriction enzyme of Bsp1286I (New England Biolabs, Ipswich, MA, USA) was employed for genotyping [21,51]. In brief, 150 ng genomic DNA of each individual sample was digested with Bsp1286I (New England Biolabs, Ipswich, MA, USA) at 37 °C for 2 h followed by the ligation of oligos as barcodes using T4 ligase (New England Biolabs, Ipswich, MA, USA) at 16 °C for 1.5 h. Both enzymes were inactivated at 65 °C for 20 min. Digested and ligated DNAs of numerous samples were pooled and purified together with a Qiaquick PCR purification kit (Qiagen, Hilden, Germany) and then AMPure XP beads (Beckman Coulter Life Sciences, Indianapolis, IN, USA). The purified products was subjected to PCR amplification with the Q5 high fidelity DNA polymerase (New England Biolabs, Ipswich, MA, USA) and the primers matching Illumina adaptors. PCR products purified using AMPure XP beads were sequenced on an Illumina HiseqX 10 platform at Novogene (Novogene, Sacramento, CA, USA), producing paired end 2 × 150 bp sequencing reads.

4.3. Genotypes of GBS Segment Markers

Illumina adaptors and low-quality sequences of raw reads were trimmed using Trimmomatic (version 0.38) [52], followed by decoding and fine trimming of customized adaptors with custom scripts to assign reads to each individual sample. To increase genotyping accuracy, whole genome sequencing (WGS) data of A188 (SRA accessions: SRR11870960 and SRR11870961) and B73 (SRA accessions: SRR4039069 and SRR4039070) were used to confirm genotypes of the two parental lines [21,53].

Reads were aligned to the B73 reference genome (B73Ref4) [54] with BWA [55]. Alignments were removed if they did not match any of the following criteria: 1. The insert size was in the range of 50–800 bp; 2. The mapping score was greater than 40; 3. The match region was greater than 50; 4. The mismatch percentage was less than 6%; and 5. The percentage of the unmatched overhang (or tail) was less than 5% of read length. SNPs were identified with GATK haplotypecaller [56,57], which were further filtered and converted to segment (bin) markers by using the R package (version 0.01) of Genomap (https://github.com/liu3zhenlab/genomap, accessed on 1 October 2021)

4.4. Genetic Mapping Using Logistic Regression

With GBS segment genotyping data of individual XT-I and XT-II samples, the logistic regression was employed to test for the null hypothesis that, at a marker site, genotype frequencies between the groups are not different. Significance thresholds were determined using two approaches: 1. Accounting for multiple tests with a false discovery rate (FDR) of 1% [58], and 2. Conducting 1000 permutation tests similar to a standard QTL permutation test to determine the distribution of *p*-values under the null hypothesis and selecting 5% as the significance *p*-value cutoff.

4.5. QTL Mapping Using R/qtl

Genetic positions of segment markers were estimated using a B73xA188 double haploid (DH) genetic map [21]. The R/qtl function scanone was used to map the QTLs with the standard interval mapping method and the binary model [59]. Two LOD thresholds were used: The LOD value at the 5% significance level from 1000 permutations and the LOD value of 3 [60]. The R/qtl function fitqtl was used to estimate the percentage of the QTL effect on the phenotype.

4.6. RNA Extraction and Sequencing of Bulked Samples

XT-I, XT-II, A188 fast- and slow-growing pooled tissue samples were ground with mortar and pestle under liquid nitrogen. RNA was isolated using the RNeasy Plant Mini Kit (Qiagen, Germantown, MD, USA) following the manufacturer's instructions. Library preparation and RNA sequencing were performed at Novogene (Novogene, Beijing, China).

4.7. BSR-seq Analysis

RNA-seq raw reads were trimmed with Trimmomatic (version 0.38) [52] and aligned to B73Ref4 with STAR (version 2.7.3a) [61]. SNPs were called using GATK UnifiedGenotyper [56,57]. Bi-allelic SNPs were selected using GATK with the criteria "AF $\geq$ 0.2 && QUAL $\geq$ 30.0 && DP $\geq$ 100 && DP < 10,000". Potential error SNPs that did not match polymorphic data between B73 and A188 were discarded. A generalized linear model assuming the binomial distribution of two alleles was employed to detect the association between each SNP and callus type.

4.8. Identification of Callus Type-Associated Genes

With read counts per gene resulting from STAR analysis, the statistical test with DESeq2 was performed to identify DEGs [62]. *p*-values were corrected to account for multiple tests with the FDR approach [58]. The genes with FDR-adjusted *p*-values smaller than 0.1 in the comparison were considered DEGs.

To identify candidate genes responsible for callus type, we focused on DEGs located within the QTL regions. Significant DEGs from the comparisons of XT-II versus XT-I and fast- versus slow-growing calli were prioritized as candidate genes.

4.9. Gene Ontology (GO) Enrichment Analysis

Gene Ontology (GO) enrichment analysis was performed using the resampling method in GOSeq [63]. Multiple testing adjustments were applied using the FDR method, with a significance threshold of FDR-adjusted *p*-values less than 0.05 [58].

4.10. Data Visualization

All figures, including QTL mapping and the genotyping segmentation of HI-II, XT-I and II samples, were plotted using custom R scripts. Heatmaps were plotted with the R package ComplexHeatmap [64]. The input data for heatmap plotting were standardized read counts per million of total reads (RPM). Standardization was achieved by subtracting the mean RPM across all samples and dividing the result by the standard deviation.

5. Conclusions

In this study, we employed two efficient genetic mapping strategies to dissect the genetic basis of callus type, Type I and Type II, derived from F2 immature embryos of the inbred lines B73 and A188, identifying five QTLs. Transcriptomic comparisons between morphologically contrasting calli revealed differentially expressed genes associated with callus development. By integrating genetic mapping with transcriptomic analysis, we identified candidate genes that may influence callus type, which can be further validated and applied to improve plant regeneration.

Supplementary Materials: The following supporting information can be downloaded at https://www.mdpi.com/article/10.3390/plants14203168/s1, Figure S1: Detailed characterization of QTL ctAB2a; Figure S2: Detailed characterization of QTL ctAB8a; Figure S3: Detailed characterization of QTL ctAB9a; Figure S4: Effect of QTL markers on chromosomes 2, 5, 6, 8, and 9; Figure S5: Genotype distribution on chromosome 3; Figure S6: Fast- and slow-growing sections from a A188 callus; Figure S7: B73 expression atlas of Zm00001d039017 (*wox9c*) from MaizeGDB.org; Figure S8: B73

expression atlas of Zm00001d043937 (*wox9b*) from MaizeGDB.org; Figure S9: B73 expression atlas of Zm00001d043131 (*myb138*) from MaizeGDB.org; Figure S10: B73 expression atlas of Zm00001d041853 (*myb8*) from MaizeGDB.org; Figure S11: Structural comparison of *wat1* alleles; Supplementary Data S1: F2 population phenotypic and genotypic data in cross format for QTL mapping; Supplementary Data S2: Genetic mapping of callus types using GBS makers and a logistic model; Supplementary Data S3: Genetic mapping of callus types using bulk segregant RNA-seq (BSR-seq); Supplementary Data S4: Differential expressed genes between Type II and Type I calli; Supplementary Data S5: Differential expressed genes between fast- and slow-growing calli; Supplementary Data S6: Differentially expressed genes within QTL regions.

Author Contributions: Y.L. (Yunjun Liu) and S.L. conceptualized experiments; G.L., Y.L. (Yan Liu), T.M.T., Y.Q. and M.Z. conducted experiments; G.L., T.M.T. and S.L. analyzed data; G.L., J.Z., G.W., H.W., S.P., M.-J.C., F.F.W., Y.L. (Yunjun Liu) and S.L. interpreted the results and wrote the manuscript. All authors have read and agreed to the published version of the manuscript.

Funding: We thank funding provided by the USDA NIFA award (2021-67013-35724) and the NSF awards (1741090, 2011500 and 2311738). This is contribution No. 25-101-J from the Kansas Agricultural Experiment Station, Manhattan, Kansas.

Data Availability Statement: Illumina sequencing data have been deposited in the Sequence Read Archive (SRA) database under accession PRJNA1192291. Scripts used in this study can be found at https://github.com/PlantG3/culturability.git (accessed on 1 December 2024).

Conflicts of Interest: S.L. is the co-founder of Data2Bio, LLC. The other authors claim no competing interests.

References

1. Altpeter, F.; Springer, N.M.; Bartley, L.E.; Blechl, A.E.; Brutnell, T.P.; Citovsky, V.; Conrad, L.J.; Gelvin, S.B.; Jackson, D.P.; Kausch, A.P.; et al. Advancing Crop Transformation in the Era of Genome Editing. *Plant Cell* **2016**, *28*, 1510–1520. [CrossRef] [PubMed]
2. Que, Q.; Elumalai, S.; Li, X.; Zhong, H.; Nalapalli, S.; Schweiner, M.; Fei, X.; Nuccio, M.; Kelliher, T.; Gu, W.; et al. Maize Transformation Technology Development for Commercial Event Generation. *Front. Plant Sci.* **2014**, *5*, 379. [CrossRef] [PubMed]
3. Armstrong, C.L.; Green, C.E.; Phillips, R.L. Development and Availability of Germplasm with High Type II Culture Formation Response. *Maize Genet. Coop. Newsl.* **1991**, *65*, 92–93.
4. Duncan, D.R.; Williams, M.E.; Zehr, B.E.; Widholm, J.M. The Production of Callus Capable of Plant Regeneration from Immature Embryos of Numerous *Zea mays* Genotypes. *Planta* **1985**, *165*, 322–332. [CrossRef]
5. Kotchoni, S.O.; Noumavo, P.A.; Adjanohoun, A.; Russo, D.P.; Dell'Angelo, J.; Gachomo, E.W.; Baba-Moussa, L. A Simple and Efficient Seed-Based Approach to Induce Callus Production from B73 Maize Genotype. *Am. J. Mol. Biol.* **2012**, *2*, 380–385. [CrossRef]
6. Cho, M.-J.; Wu, E.; Kwan, J.; Yu, M.; Banh, J.; Linn, W.; Anand, A.; Li, Z.; TeRonde, S.; Register, J.C., 3rd; et al. Agrobacterium-Mediated High-Frequency Transformation of an Elite Commercial Maize (*Zea mays* L.) Inbred Line. *Plant Cell Rep.* **2014**, *33*, 1767–1777. [CrossRef]
7. Cho, M.-J.; Banh, J.; Yu, M.; Kwan, J.; Jones, T.J. Improvement of Agrobacterium-Mediated Transformation Frequency in Multiple Modern Elite Commercial Maize (*Zea mays* L.) Inbreds by Media Modifications. *Plant Cell Tissue Organ. Cult.* **2015**, *121*, 519–529. [CrossRef]
8. Lowe, K.; Wu, E.; Wang, N.; Hoerster, G.; Hastings, C.; Cho, M.-J.; Scelonge, C.; Lenderts, B.; Chamberlin, M.; Cushatt, J.; et al. Morphogenic Regulators Baby Boom and Wuschel Improve Monocot Transformation. *Plant Cell* **2016**, *28*, 1998–2015. [CrossRef]
9. Wang, K.; Shi, L.; Liang, X.; Zhao, P.; Wang, W.; Liu, J.; Chang, Y.; Hiei, Y.; Yanagihara, C.; Du, L.; et al. The Gene TaWOX5 Overcomes Genotype Dependency in Wheat Genetic Transformation. *Nat. Plants* **2022**, *8*, 110–117. [CrossRef]
10. Debernardi, J.M.; Tricoli, D.M.; Ercoli, M.F.; Hayta, S.; Ronald, P.; Palatnik, J.F.; Dubcovsky, J. A GRF–GIF Chimeric Protein Improves the Regeneration Efficiency of Transgenic Plants. *Nat. Biotechnol.* **2020**, *38*, 1274–1279. [CrossRef]
11. Tomes, D.T.; Smith, O.S. The Effect of Parental Genotype on Initiation of Embryogenic Callus from Elite Maize (*Zea mays* L.) Germplasm. *Theor. Appl. Genet.* **1985**, *70*, 505–509. [CrossRef]
12. Hodges, T.K.; Kamo, K.K.; Imbrie, C.W.; Becwar, M.R. Genotype Specificity of Somatic Embryogenesis and Regeneration in Maize. *Nat. Biotechnol.* **1986**, *4*, 219–223. [CrossRef]
13. Welter, M.E.; Clayton, D.S.; Miller, M.A.; EPetolino, J. Morphotypes of Friable Embryogenic Maize Callus. *Plant Cell Rep.* **1995**, *14*, 725–729. [CrossRef] [PubMed]

14. Frame, B.R.; Zhang, H.; Cocciolone, S.M.; Sidorenko, L.V.; Dietrich, C.R.; Pegg, S.E.; Zhen, S.; Schnable, P.S.; Wang, K. Production of Transgenic Maize from Bombarded Type II Callus: Effect of Gold Particle Size and Callus Morphology on Transformation Efficiency. *Vitr. Cell. Dev. Biol. Plant* **2000**, *36*, 21–29. [CrossRef]
15. D'Halluin, K.; Bonne, E.; Bossut, M.; De Beuckeleer, M.; Leemans, J. Transgenic Maize Plants by Tissue Electroporation. *Plant Cell* **1992**, *4*, 1495–1505. [PubMed]
16. Armstrong, C.L.; Green, C.E. Establishment and Maintenance of Friable, Embryogenic Maize Callus and the Involvement of L-Proline. *Planta* **1985**, *164*, 207–214. [CrossRef]
17. Kausch, A.P.; Wang, K.; Kaeppler, H.F.; Gordon-Kamm, W. Maize Transformation: History, Progress, and Perspectives. *Mol. Breed.* **2021**, *41*, 38. [CrossRef]
18. McCain, J.W.; Kamo, K.K.; Hodges, T.K. Characterization of Somatic Embryo Development and Plant Regeneration from Friable Maize Callus Cultures. *Bot. Gaz.* **1988**, *149*, 16–20. [CrossRef]
19. Ishida, Y.; Saito, H.; Ohta, S.; Hiei, Y.; Komari, T.; Kumashiro, T. High Efficiency Transformation of Maize (*Zea mays* L.) Mediated by Agrobacterium Tumefaciens. *Nat. Biotechnol.* **1996**, *14*, 745–750. [CrossRef]
20. Songstad, D.D.; Armstrong, C.L.; Petersen, W.L.; Hairston, B.; Hinchee, M.A.W. Production of Transgenic Maize Plants and Progeny by Bombardment of Hi-II Immature Embryos. *Vitr. Cell. Dev. Biol. Plant* **1996**, *32*, 179–183. [CrossRef]
21. Lin, G.; He, C.; Zheng, J.; Koo, D.-H.; Le, H.; Zheng, H.; Tamang, T.M.; Lin, J.; Liu, Y.; Zhao, M.; et al. Chromosome-Level Genome Assembly of a Regenerable Maize Inbred Line A188. *Genome Biol.* **2021**, *22*, 175. [CrossRef]
22. Armstrong, C.L.; Romero-Severson, J.; Hodges, T.K. Improved Tissue Culture Response of an Elite Maize Inbred through Backcross Breeding, and Identification of Chromosomal Regions Important for Regeneration by RFLP Analysis. *Züchter Genet. Breed. Res.* **1992**, *84*, 755–762. [CrossRef] [PubMed]
23. Lowe, B.A.; Way, M.M.; Kumpf, J.M.; Rout, J.; Warner, D.; Johnson, R.; Armstrong, C.L.; Spencer, M.T.; Chomet, P.S. Marker Assisted Breeding for Transformability in Maize. *Mol. Breed.* **2006**, *18*, 229–239. [CrossRef]
24. Krakowsky, M.D.; Lee, M.; Garay, L.; Woodman-Clikeman, W.; Long, M.J.; Sharopova, N.; Frame, B.; Wang, K. Quantitative Trait Loci for Callus Initiation and Totipotency in Maize (*Zea mays* L.). *Züchter Genet. Breed. Res.* **2006**, *113*, 821–830. [CrossRef]
25. Salvo, S.; Cook, J.; Carlson, A.R.; Hirsch, C.N.; Kaeppler, S.M.; Kaeppler, H.F. Genetic Fine-Mapping of a Quantitative Trait Locus (QTL) Associated with Embryogenic Tissue Culture Response and Plant Regeneration Ability in Maize (*Zea mays* L.). *Plant Genome* **2018**, *11*, 170111. [CrossRef] [PubMed]
26. McFarland, F.L.; Collier, R.; Walter, N.; Martinell, B.; Kaeppler, S.M.; Kaeppler, H.F. A Key to Totipotency: Wuschel-like Homeobox 2a Unlocks Embryogenic Culture Response in Maize (*Zea mays* L.). *Plant Biotechnol. J.* **2023**, *21*, 1860–1872. [CrossRef]
27. Chu, C.C. Establishment of an Efficient Medium for Anther Culture of Rice through Comparative Experiments on the Nitrogen Sources. *Sci. Sin.* **1975**, *18*, 659–668.
28. Ren, W.; Gong, X.; Li, K.; Zhang, H.; Chen, F.; Pan, Q. Recombination Pattern Characterization via Simulation Using Different Maize Populations. *Int. J. Mol. Sci.* **2020**, *21*, 2222. [CrossRef]
29. Hoopes, G.M.; Hamilton, J.P.; Wood, J.C.; Esteban, E.; Pasha, A.; Vaillancourt, B.; Provart, N.J.; Buell, C.R. An Updated Gene Atlas for Maize Reveals Organ-Specific and Stress-Induced Genes. *Plant J.* **2019**, *97*, 1154–1167. [CrossRef]
30. Stelpflug, S.C.; Sekhon, R.S.; Vaillancourt, B.; Hirsch, C.N.; Robin Buell, C.; de Leon, N.; Kaeppler, S.M. An Expanded Maize Gene Expression Atlas Based on RNA Sequencing and Its Use to Explore Root Development. *Plant Genome* **2016**, *9*, plantgenome2015.04.0025. [CrossRef]
31. Li, L.; Li, D.; Liu, S.; Ma, X.; Dietrich, C.R.; Hu, H.-C.; Zhang, G.; Liu, Z.; Zheng, J.; Wang, G.; et al. The Maize glossy13 Gene, Cloned via BSR-Seq and Seq-Walking Encodes a Putative ABC Transporter Required for the Normal Accumulation of Epicuticular Waxes. *PLoS ONE* **2013**, *8*, e82333. [CrossRef]
32. Zheng, J.; He, C.; Qin, Y.; Lin, G.; Park, W.D.; Sun, M. Co-expression Analysis Aids in the Identification of Genes in the Cuticular Wax Pathway in Maize. *Plant J.* **2019**, *97*, 530–542. [CrossRef]
33. Lewandowska, M.; Keyl, A.; Feussner, I. Wax Biosynthesis in Response to Danger: Its Regulation upon Abiotic and Biotic Stress. *New Phytol.* **2020**, *227*, 698–713. [CrossRef] [PubMed]
34. Shen, G.; Sun, W.; Chen, Z.; Shi, L.; Hong, J.; Shi, J. Plant GDSL Esterases/Lipases: Evolutionary, Physiological and Molecular Functions in Plant Development. *Plants* **2022**, *11*, 468. [CrossRef] [PubMed]
35. Liu, H.; Adesina, O.; Bika, R.; Singh, R.; Jugulam, M.; Liu, S. Homotools: A Suite of Genomic Tools for Homologous Retrieval and Comparison. *Genom. Commun.* **2024**, *1*, e002. [CrossRef]
36. Ranocha, P.; Denancé, N.; Vanholme, R.; Freydier, A.; Martinez, Y.; Hoffmann, L.; Köhler, L.; Pouzet, C.; Renou, J.-P.; Sundberg, B.; et al. Walls Are Thin 1 (WAT1), an Arabidopsis Homolog of Medicago Truncatula NODULIN21, Is a Tonoplast-Localized Protein Required for Secondary Wall Formation in Fibers. *Plant J.* **2010**, *63*, 469–483. [CrossRef]
37. Koseoglou, E.; Hanika, K.; Mohd Nadzir, M.M.; Kohlen, W.; van der Wolf, J.M.; Visser, R.G.F.; Bai, Y. Inactivation of Tomato WAT1 Leads to Reduced Susceptibility to Clavibacter Michiganensis through Downregulation of Bacterial Virulence Factors. *Front. Plant Sci.* **2023**, *14*, 1082094. [CrossRef]

38. Marowa, P.; Ding, A.; Kong, Y. Expansins: Roles in Plant Growth and Potential Applications in Crop Improvement. *Plant Cell Rep.* **2016**, *35*, 949–965. [CrossRef]
39. Shen, Y.; Jiang, Z.; Yao, X.; Zhang, Z.; Lin, H.; Zhao, M.; Liu, H.; Peng, H.; Li, S.; Pan, G. Genome Expression Profile Analysis of the Immature Maize Embryo during Dedifferentiation. *PLoS ONE* **2012**, *7*, e32237. [CrossRef]
40. Nishikubo, N.; Takahashi, J.; Roos, A.A.; Derba-Maceluch, M.; Piens, K.; Brumer, H.; Teeri, T.T.; Stålbrand, H.; Mellerowicz, E.J. Xyloglucan Endo-Transglycosylase-Mediated Xyloglucan Rearrangements in Developing Wood of Hybrid Aspen. *Plant Physiol.* **2011**, *155*, 399–413. [CrossRef]
41. Wormit, A.; Usadel, B. The Multifaceted Role of Pectin Methylesterase Inhibitors (PMEIs). *Int. J. Mol. Sci.* **2018**, *19*, 2878. [CrossRef] [PubMed]
42. Ge, F.; Luo, X.; Huang, X.; Zhang, Y.; He, X.; Liu, M.; Lin, H.; Peng, H.; Li, L.; Zhang, Z.; et al. Genome-Wide Analysis of Transcription Factors Involved in Maize Embryonic Callus Formation. *Physiol. Plant.* **2016**, *158*, 452–462. [CrossRef] [PubMed]
43. Ikeuchi, M.; Favero, D.S.; Sakamoto, Y.; Iwase, A.; Coleman, D.; Rymen, B.; Sugimoto, K. Molecular Mechanisms of Plant Regeneration. *Annu. Rev. Plant Biol.* **2019**, *70*, 377–406. [CrossRef] [PubMed]
44. Kim, J.; Jung, J.H.; Lee, S.B.; Go, Y.S.; Kim, H.J.; Cahoon, R.; Markham, J.E.; Cahoon, E.B.; Suh, M.C. Arabidopsis 3-Ketoacyl-Coenzyme a synthase9 Is Involved in the Synthesis of Tetracosanoic Acids as Precursors of Cuticular Waxes, Suberins, Sphingolipids, and Phospholipids. *Plant Physiol.* **2013**, *162*, 567–580. [CrossRef]
45. Liu, S.; Dietrich, C.R.; Schnable, P.S. DLA-Based Strategies for Cloning Insertion Mutants: Cloning the gl4 Locus of Maize Using Mu Transposon Tagged Alleles. *Genetics* **2009**, *183*, 1215–1225. [CrossRef]
46. Shang, B.; Xu, C.; Zhang, X.; Cao, H.; Xin, W.; Hu, Y. Very-Long-Chain Fatty Acids Restrict Regeneration Capacity by Confining Pericycle Competence for Callus Formation in Arabidopsis. *Proc. Natl. Acad. Sci. USA* **2016**, *113*, 5101–5106. [CrossRef]
47. Nobusawa, T.; Okushima, Y.; Nagata, N.; Kojima, M.; Sakakibara, H.; Umeda, M. Synthesis of Very-Long-Chain Fatty Acids in the Epidermis Controls Plant Organ Growth by Restricting Cell Proliferation. *PLoS Biol.* **2013**, *11*, e1001531. [CrossRef]
48. Qin, Y.-M.; Hu, C.-Y.; Pang, Y.; Kastaniotis, A.J.; Hiltunen, J.K.; Zhu, Y.-X. Saturated Very-Long-Chain Fatty Acids Promote Cotton Fiber and Arabidopsis Cell Elongation by Activating Ethylene Biosynthesis. *Plant Cell* **2007**, *19*, 3692–3704. [CrossRef]
49. Frame, B.R.; McMurray, J.M.; Fonger, T.M.; Main, M.L.; Taylor, K.W.; Torney, F.J.; Paz, M.M.; Wang, K. Improved Agrobacterium-Mediated Transformation of Three Maize Inbred Lines Using MS Salts. *Plant Cell Rep.* **2006**, *25*, 1024–1034. [CrossRef]
50. Liu, S.; Yeh, C.-T.; Tang, H.M.; Nettleton, D.; Schnable, P.S. Gene Mapping via Bulked Segregant RNA-Seq (BSR-Seq). *PLoS ONE* **2012**, *7*, e36406. [CrossRef]
51. Ott, A.; Liu, S.; Schnable, J.C.; Yeh, C.T.E. tGBS® Genotyping-by-Sequencing Enables Reliable Genotyping of Heterozygous Loci. *Nucleic Acids* **2017**, *45*, e178. [CrossRef]
52. Bolger, A.M.; Lohse, M.; Usadel, B. Trimmomatic: A Flexible Trimmer for Illumina Sequence Data. *Bioinformatics* **2014**, *30*, 2114–2120. [CrossRef]
53. Liu, S.; Zheng, J.; Migeon, P.; Ren, J.; Hu, Y.; He, C.; Liu, H.; Fu, J.; White, F.F.; Toomajian, C.; et al. Unbiased K-Mer Analysis Reveals Changes in Copy Number of Highly Repetitive Sequences During Maize Domestication and Improvement. *Sci. Rep.* **2017**, *7*, 42444. [CrossRef] [PubMed]
54. Jiao, Y.; Peluso, P.; Shi, J.; Liang, T.; Stitzer, M.C.; Wang, B.; Campbell, M.S.; Stein, J.C.; Wei, X.; Chin, C.-S.; et al. Improved Maize Reference Genome with Single-Molecule Technologies. *Nature* **2017**, *546*, 524–527. [CrossRef] [PubMed]
55. Li, H.; Durbin, R. Fast and Accurate Long-Read Alignment with Burrows-Wheeler Transform. *Bioinformatics* **2010**, *26*, 589–595. [CrossRef] [PubMed]
56. McKenna, A.; Hanna, M.; Banks, E.; Sivachenko, A.; Cibulskis, K.; Kernytsky, A.; Garimella, K.; Altshuler, D.; Gabriel, S.; Daly, M.; et al. The Genome Analysis Toolkit: A MapReduce Framework for Analyzing next-Generation DNA Sequencing Data. *Genome Res.* **2010**, *20*, 1297–1303. [CrossRef]
57. Poplin, R.; Ruano-Rubio, V.; DePristo, M.A.; Fennell, T.J.; Carneiro, M.O.; Van der Auwera, G.A.; Kling, D.E.; Gauthier, L.D.; Levy-Moonshine, A.; Roazen, D.; et al. Scaling Accurate Genetic Variant Discovery to Tens of Thousands of Samples. *bioRxiv.* **2018**, 201178. [CrossRef]
58. Benjamini, Y.; Hochberg, Y. Controlling the False Discovery Rate: A Practical and Powerful Approach to Multiple Testing. *J. R. Stat. Soc.* **1995**, *57*, 289–300. [CrossRef]
59. Broman, K.W.; Wu, H.; Sen, S.; Churchill, G.A. R/qtl: QTL Mapping in Experimental Crosses. *Bioinformatics* **2003**, *19*, 889–890. [CrossRef]
60. Broman, K.W. Review of Statistical Methods for QTL Mapping in Experimental Crosses. *Lab Anim.* **2001**, *30*, 44–52.
61. Dobin, A.; Davis, C.A.; Schlesinger, F.; Drenkow, J.; Zaleski, C.; Jha, S.; Batut, P.; Chaisson, M.; Gingeras, T.R. STAR: Ultrafast Universal RNA-Seq Aligner. *Bioinformatics* **2013**, *29*, 15–21. [CrossRef]
62. Love, M.I.; Huber, W.; Anders, S. Moderated Estimation of Fold Change and Dispersion for RNA-Seq Data with DESeq2. *Genome Biol.* **2014**, *15*, 550. [CrossRef]

63. Young, M.D.; Wakefield, M.J.; Smyth, G.K.; Oshlack, A. Gene Ontology Analysis for RNA-Seq: Accounting for Selection Bias. *Genome Biol.* **2010**, *11*, R14. [CrossRef]
64. Gu, Z.; Eils, R.; Schlesner, M. Complex Heatmaps Reveal Patterns and Correlations in Multidimensional Genomic Data. *Bioinformatics* **2016**, *32*, 2847–2849. [CrossRef]

Disclaimer/Publisher's Note: The statements, opinions and data contained in all publications are solely those of the individual author(s) and contributor(s) and not of MDPI and/or the editor(s). MDPI and/or the editor(s) disclaim responsibility for any injury to people or property resulting from any ideas, methods, instructions or products referred to in the content.